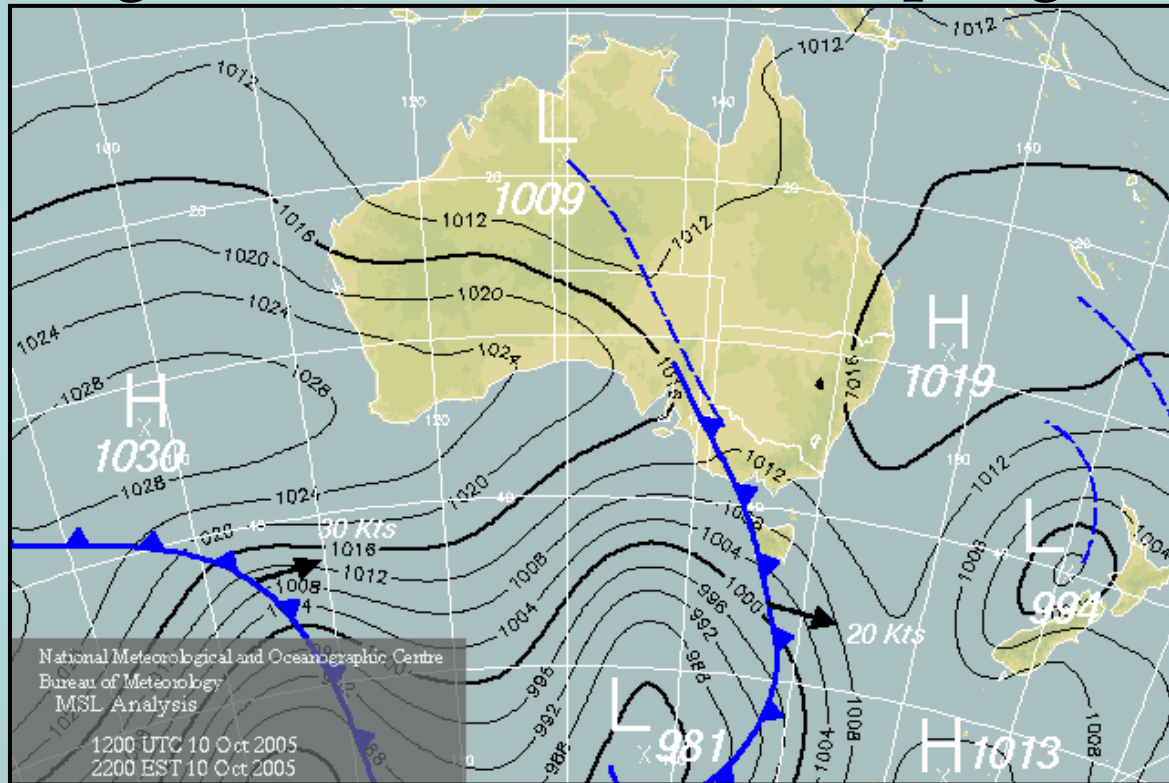


The dynamics of heat lows over flat terrain

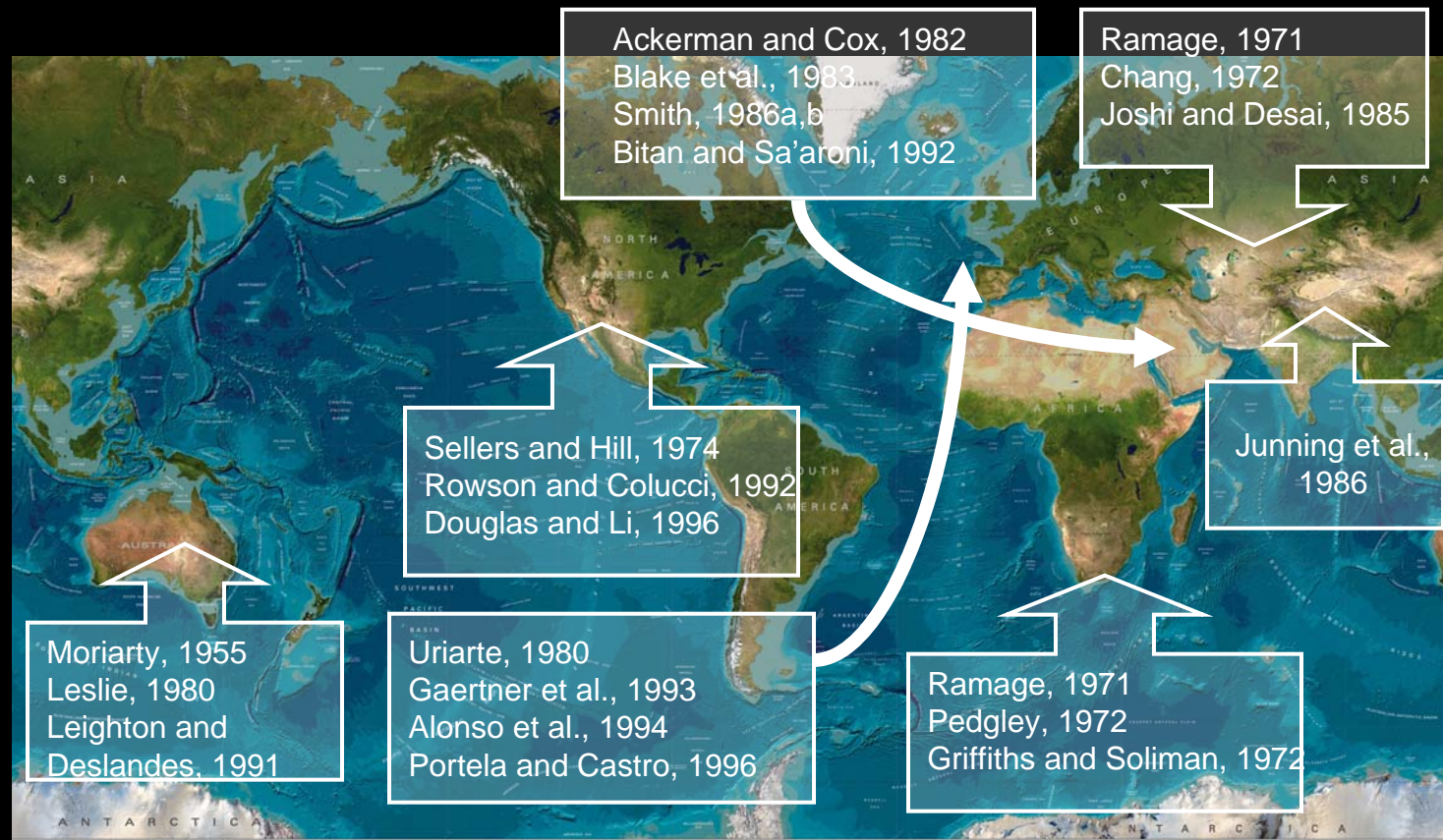
Roger K. Smith , Thomas Spengler



presented by **Julia Palamarchuk**, Ukraine, Odessa

Split Workshop in Atmospheric Physics and Oceanography, May 22-30, Split, Croatia

Previous Investigations



www.qebco.net/data_and_products/qebco_world_map/

Modelling studies of heat lows ...

Leslie, 1980;
Fandry and Leslie, 1984;
Kepert and Smith, 1992;
Gaertner *et al.*, 1993;

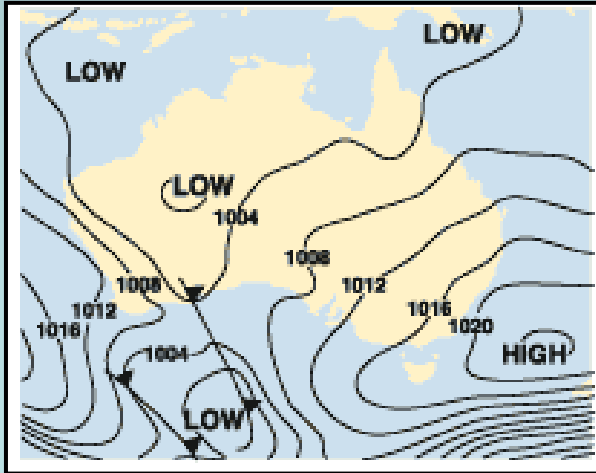
Adams, 1986, 1993;
Rácz and Smith, 1999;
Reichmann and Smith, 2003;
Spengler *et al.*, 2005;

Zängl and Chico, 2006;
Leslie and Skinner, 1994;
Alonso *et al.*, 1994;
Portela and Castro, 1996;
Hoinka and Castro, 2003.

Definition and Main Findings

(Rácz and Smith, 1999, henceforth RS99)

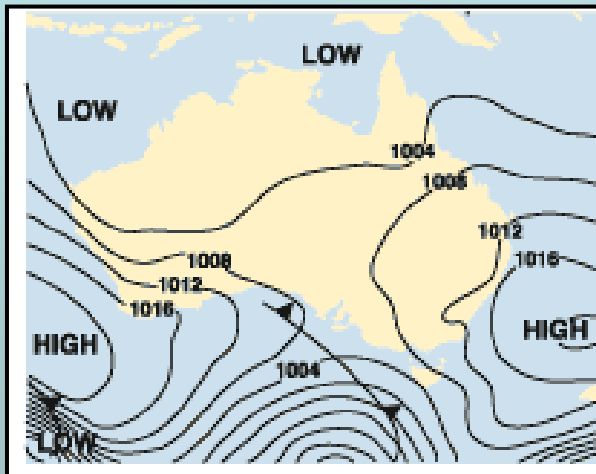
Heat Low (HL)



• HL has a minimum surface pressure in the late afternoon or early evening, while relative vorticity is strongest in early morning. So, HL is not approximately in quasi-geostrophic balance.

• The low-level convergence is associated with the sea breeze and nocturnal low-level jet.

Heat Trough



• HL is characterized by an anticyclonic PV anomaly relative to its environment on account of greatly reduced static stability in the convectively well-mixed boundary layer.

• The horizontal components of relative vorticity and horizontal potential temperature gradient make a non-negligible contribution to the PV in certain flow regions.

Conclusions

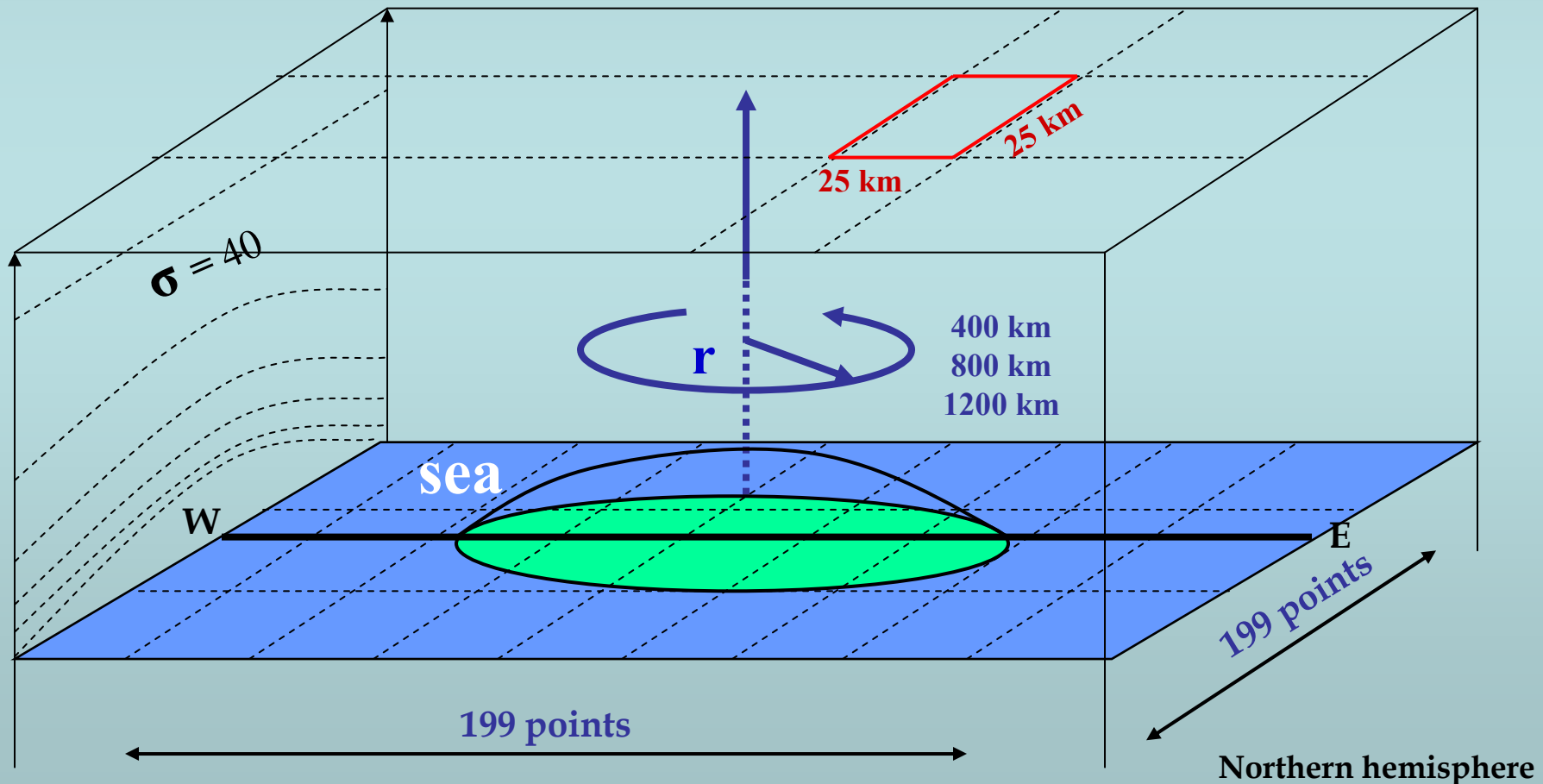
1. Implementation of corrected and extended version of radiation scheme leads to a more realistic depth of the daytime mixed layer.
2. The upper-level anticyclone extends through much of the troposphere, but has a maximum strength in the lower troposphere.
3. The anticyclone develops steadily over a period of a few days and is associated with the return branch of sea-breeze circulation in lower troposphere and slow diurnal-mean outflow in the middle and upper troposphere.
4. The upper anticyclone is largely in gradient wind balance.
5. The gravity wave has a significant effect on the radial and vertical components of motion field at any one time.
6. In a mean sense we can distinguish between distinct patterns of the tangential flow component
 - between midnight and noon, when the low-level cyclone is strongest, and
 - between noon and midnight when it is much weaker.

The Basic Model Features for the Heat Low

Modified version of hydrostatic primitive-equation model described by Rácz and Smith, 1999.

Main changes :

- implementation of radiation scheme;
- relaxation scheme for the horizontal BC;
- 10 additional upper model levels with increased horizontal diffusion.



Radiation Scheme (Raymond (1994))

Equivalent potential temperature tendency

$$\frac{d\theta_e}{dt} = L + \dot{R} \quad (1)$$

θ_e - equivalent potential temperature,
 L - relaxation to a background state of the atmosphere,
 \dot{R} - radiative heating rate.

$$\dot{R} = \frac{\theta_e}{\rho c_p T} (Q_{\text{sol}} + Q_{\text{therm}}) \quad (2)$$

Q_{sol} , Q_{therm} - contributions due to the absorption of solar and long-wave radiation, respectively.

$$Q_{\text{sol}} = \epsilon \cos \alpha Q_{\text{max}} \exp \left\{ - \left(\frac{z - z_{\text{max}}}{z_w} \right)^2 \right\} \quad (3)$$

ϵ - measure of fraction of clear sky, ($\epsilon = 1$)
 $\cos(\alpha)$ - cosine of the zenith angle of the sun,
 Q_{max} - maximum heating rate,
 z_{max} - height (fixed) of maximum heating,
 z_w - fixed height.

$$\frac{d\theta}{dt} = \dot{R} = \frac{\theta}{\rho c_p T} Q_{\text{therm}} + \frac{\theta}{T} Q_{\text{sol}} \quad (4)$$

$$Q_{\text{sol}} = \epsilon \cos \alpha \left[Q_{\text{max}}^t \exp \left\{ - \left(\frac{z - z_{\text{max}}^t}{z_w^t} \right)^2 \right\} + Q_{\text{max}}^s \exp \left\{ - \left(\frac{z - z_{\text{max}}^s}{z_w^s} \right)^2 \right\} \right] \quad (5)$$

t and s indicate the values corresponding to the troposphere or stratosphere, respectively.

Parameters used in equation (5)

Parameter	Value
Q_{max}^t	$3.5 \times 10^{-5} \text{ K s}^{-1} \approx 3 \text{ K day}^{-1}$
z_{max}^t	$3 \times 10^3 \text{ m}$
z_w^t	$4 \times 10^3 \text{ m}$
Q_{max}^s	$5 \times 10^{-4} \text{ K s}^{-1} \approx 43 \text{ K day}^{-1}$
z_{max}^s	$5 \times 10^4 \text{ m}$
z_w^s	$1.8 \times 10^4 \text{ m}$

Radiation Scheme

In a gray-atmosphere model for the thermal radiation

$$Q_{\text{therm}} = -\frac{d}{dz} (I^+ - I^-) \quad (6)$$

I^+ , I^- - upward and downward radiances.

$$\mu(z) = \mu_0 + \mu_1 \exp(-z/H) \quad (9)$$

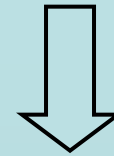
$$\begin{aligned} H &= 7000 \text{ m,} \\ \mu_0 &= 4.0 \times 10^{-4} \text{ m}^2/\text{kg,} \\ \mu_1 &= 3.0 \times 10^{-4} \text{ m}^2/\text{kg.} \end{aligned}$$

With the Schwarzschild-Schuster approximation

$$\frac{dI^+}{dz} = \rho\mu(\sigma_{\text{sb}}T^4 - I^+) \quad (7)$$

$$\frac{dI^-}{dz} = -\rho\mu(\sigma_{\text{sb}}T^4 - I^-) \quad (8)$$

μ - effective absorptivity of the atmosphere
in the infrared,
 σ_{sb} - the Stefan-Boltzmann constant.



$$Q_{\text{therm}} = -\rho\mu (2\sigma_{\text{sb}}T^4 - I^+ - I^-) \quad (10)$$

At the top of domain :

a) assumed radiative equilibrium

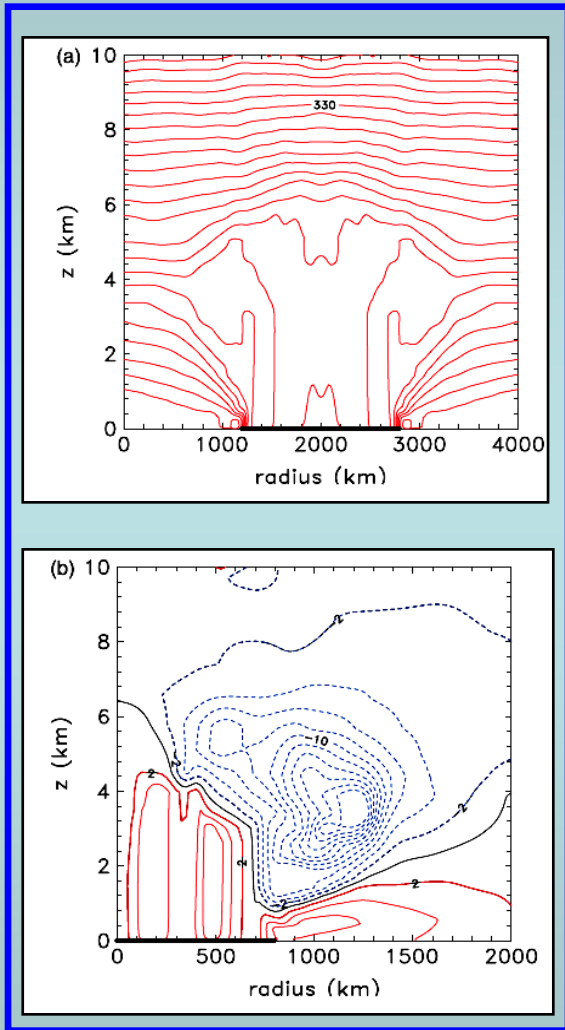
$I^- = 0$ replaced by $d\theta/dt = 0$,

b) $T = 230 \text{ K}$ at $P = 0.7 \text{ hPa}$.

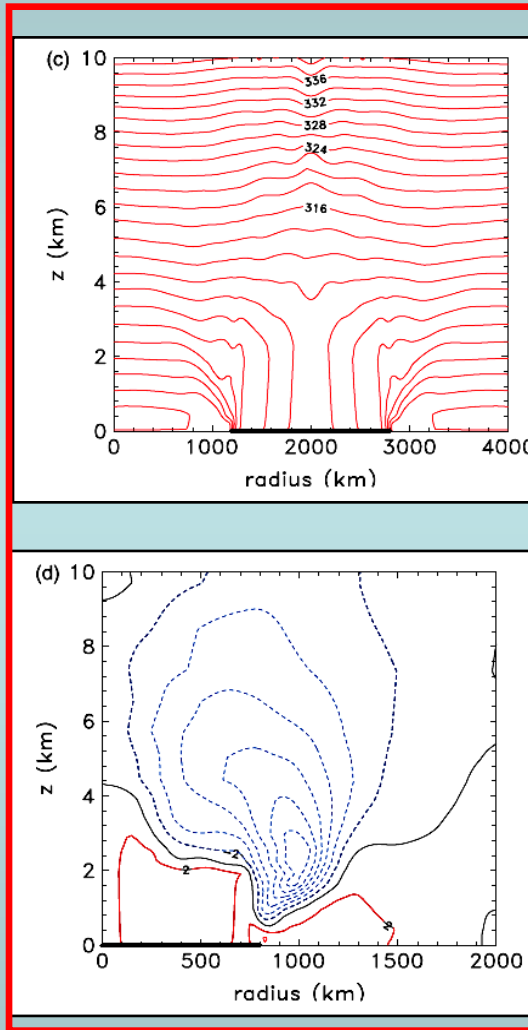
Impact of Radiation Scheme

Without radiation scheme

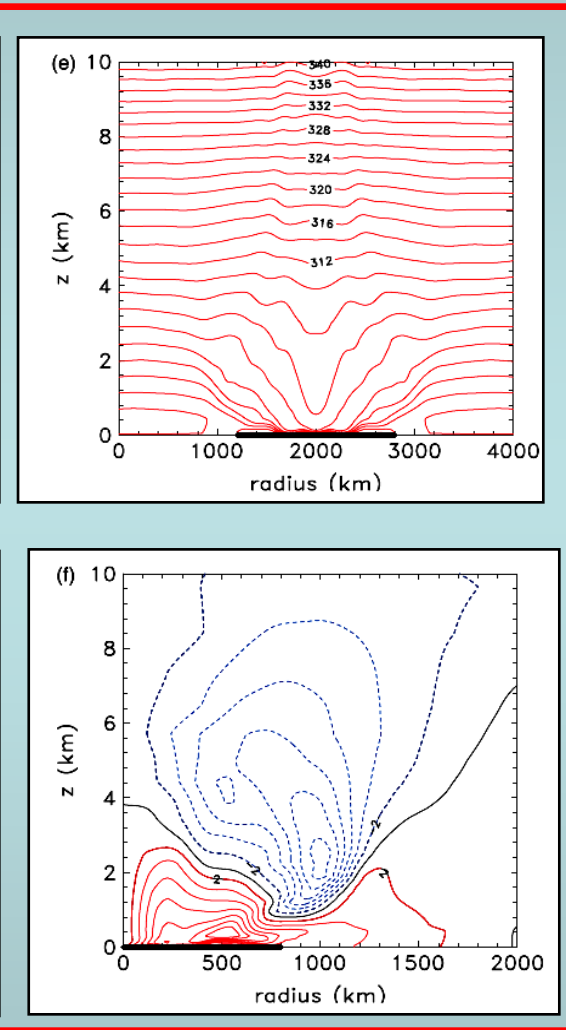
With new radiation scheme



17.00 h



17.00 h



05.00 h

θ ,
Potential
Temperature
(2 K)

V ,
Tangential
Wind
Component
(2 m/s)

Solid lines - Z_n , dashed lines - A_z circulations.

Conclusions

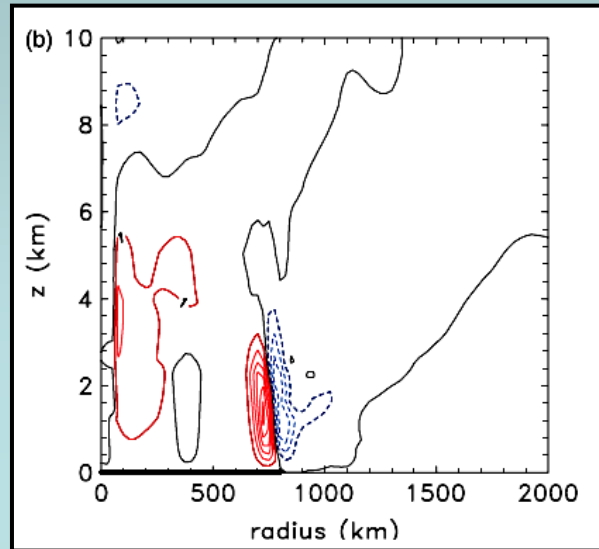
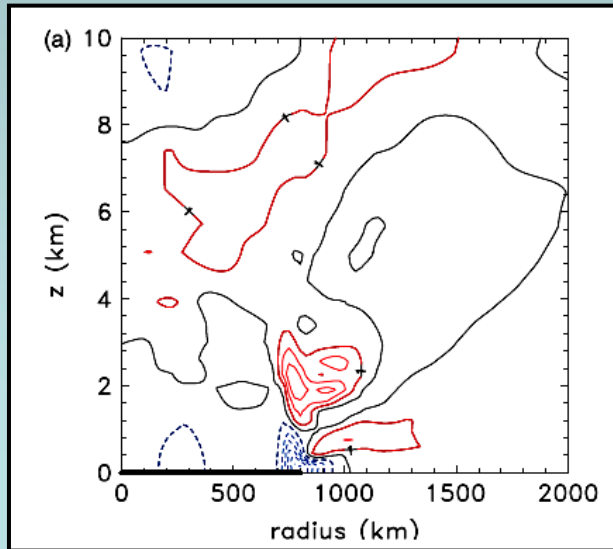
1. Implementation of corrected and extended version of radiation scheme leads to a more realistic depth of the daytime mixed layer.
2. The upper-level anticyclone extends through much of the troposphere, but has a maximum strength in the lower troposphere.
3. The anticyclone develops steadily over a period of a few days and is associated with the return branch of sea-breeze circulation in lower troposphere and slow diurnal-mean outflow in the middle and upper troposphere.
4. The upper anticyclone is largely in gradient wind balance.
5. The gravity wave has a significant effect on the radial and vertical components of motion field at any one time.
6. In a mean sense we can distinguish between distinct patterns of the tangential flow component
 - between midnight and noon, when the low-level cyclone is strongest, and
 - between noon and midnight when it is much weaker.

Impact of Radiation Scheme

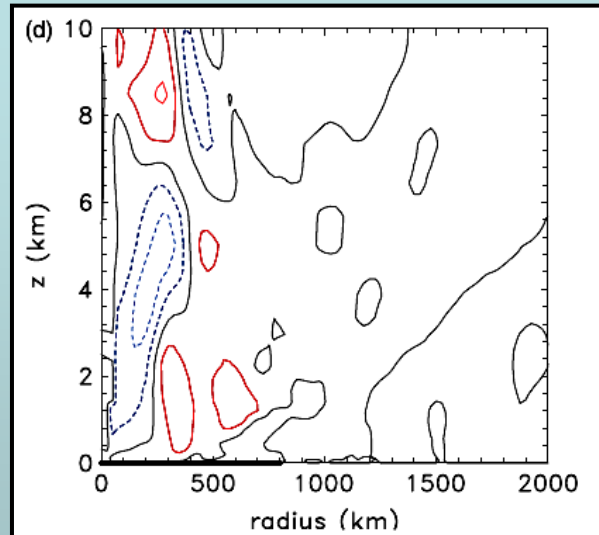
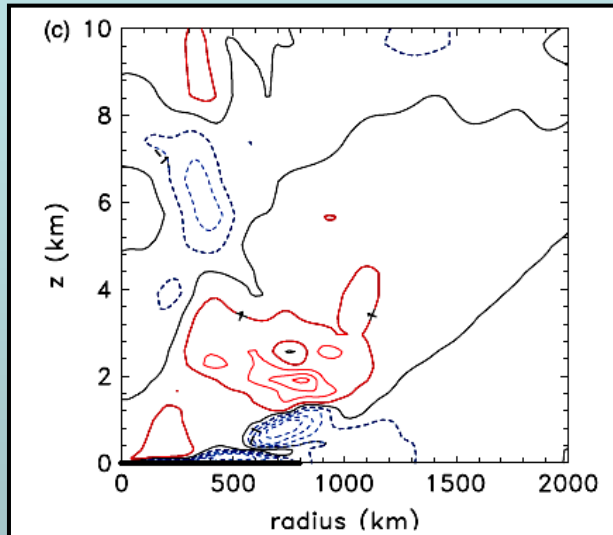
Radial wind speed, contour 1 m/s

Vertical velocity, contour 2 cm/s

17.00 h



05.00 h



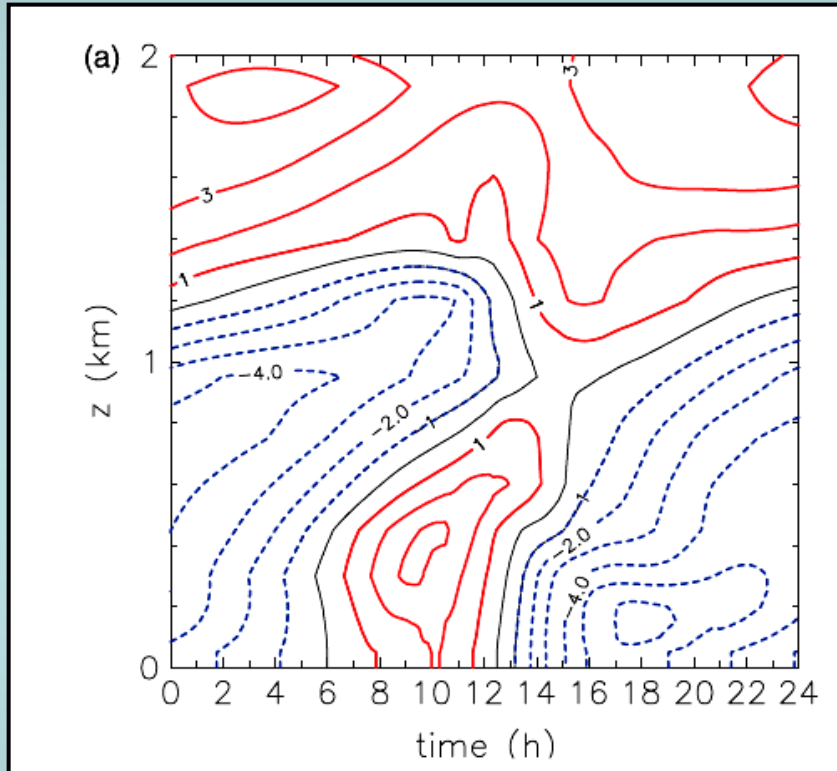
Solid lines - outward,
dashed lines - inward flow.

Solid lines - upward,
dashed lines - downward flow.

Impact of Radiation Scheme

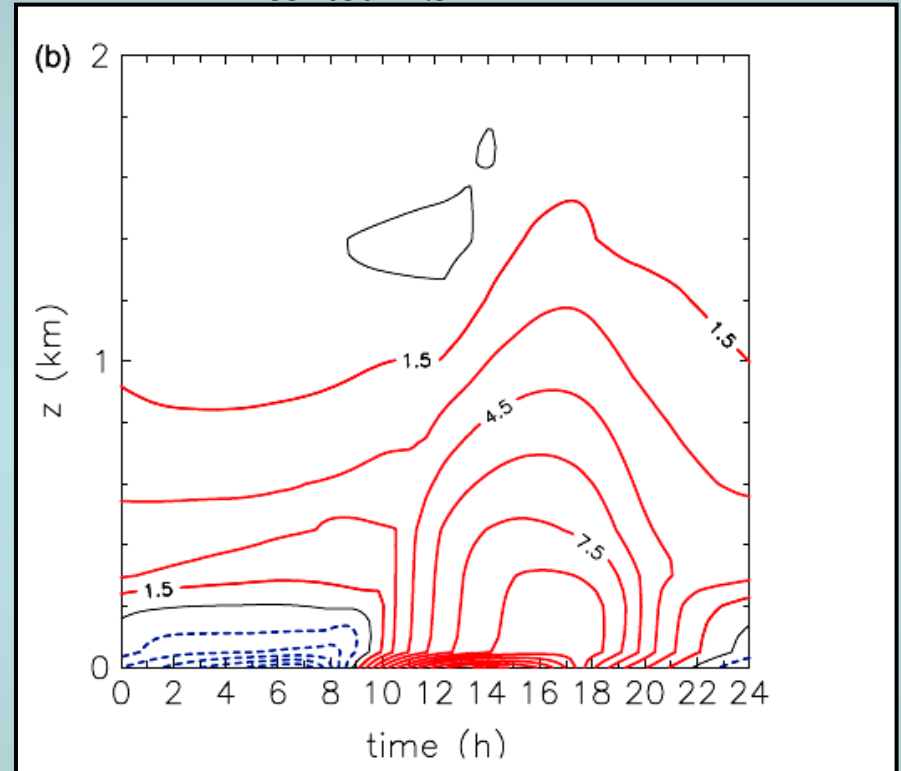
Evolution in time

Radial wind speed, contour 1 m/s



Solid lines - offshore,
dashed lines - onshore flow.

Difference of potential temperature, contour 1.5 K



$(\theta_{\text{inland}} - \theta_{\text{offshore}})$

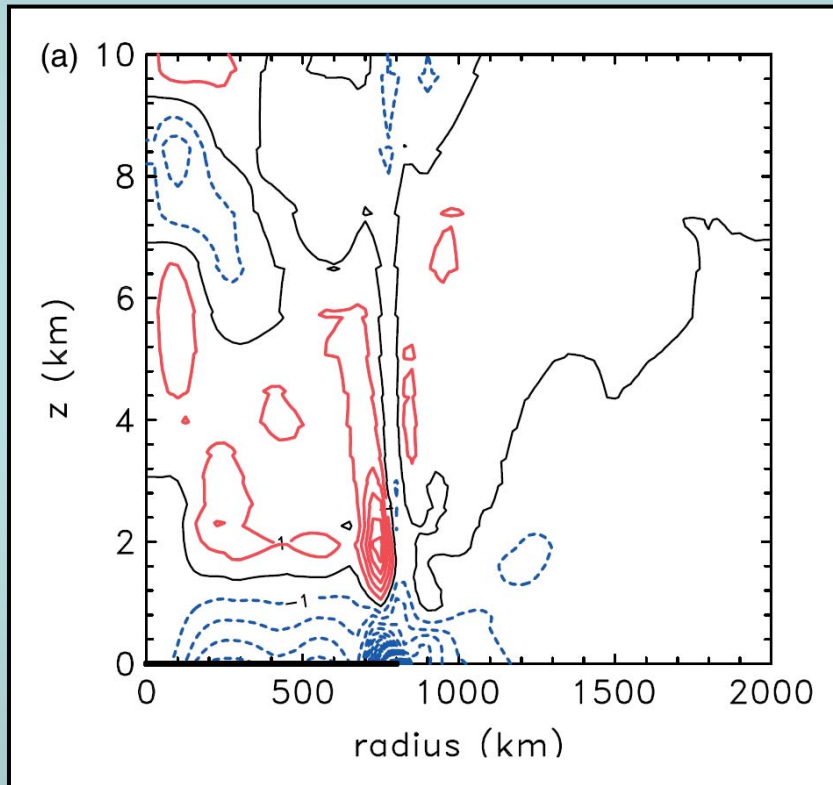
Conclusions

1. Implementation of corrected and extended version of radiation scheme leads to a more realistic depth of the daytime mixed layer.
2. The upper-level anticyclone extends through much of the troposphere, but has a maximum strength in the lower troposphere.
3. The anticyclone develops steadily over a period of a few days and is associated with the return branch of sea-breeze circulation in lower troposphere and slow diurnal-mean outflow in the middle and upper troposphere.
4. The upper anticyclone is largely in gradient wind balance.
5. The gravity wave has a significant effect on the radial and vertical components of motion field at any one time.
6. In a mean sense we can distinguish between distinct patterns of the tangential flow component
 - between midnight and noon, when the low-level cyclone is strongest, and
 - between noon and midnight when it is much weaker.

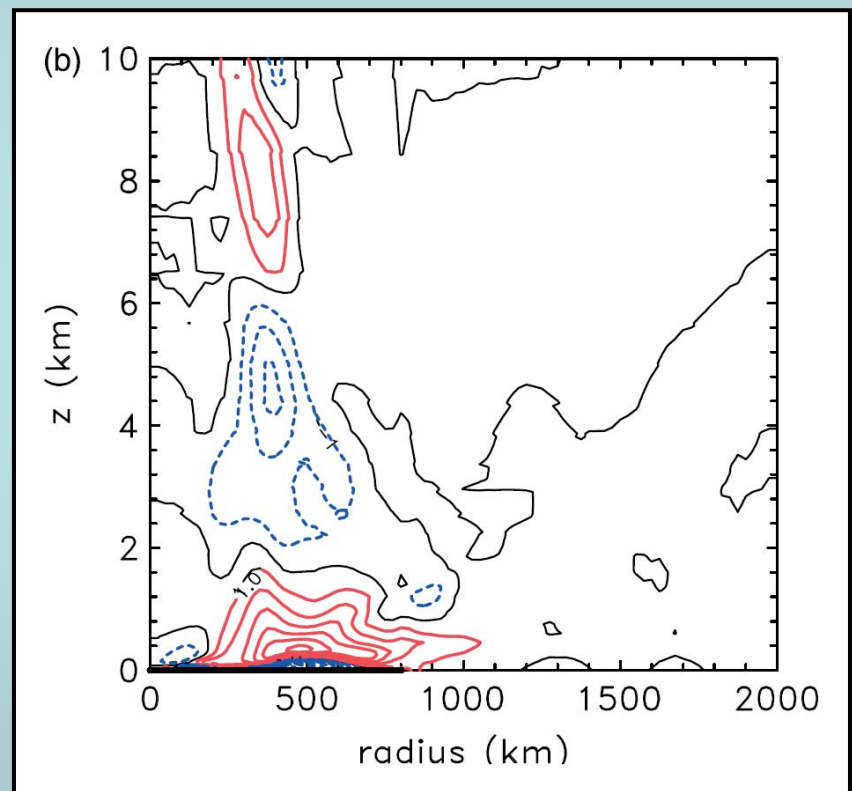
Balanced Diagnostics

Vertical cross-sections of unbalanced pressure gradient force per unit mass, contour $5 \times 10^{-5} \text{ m/s}^2$

17.00 h



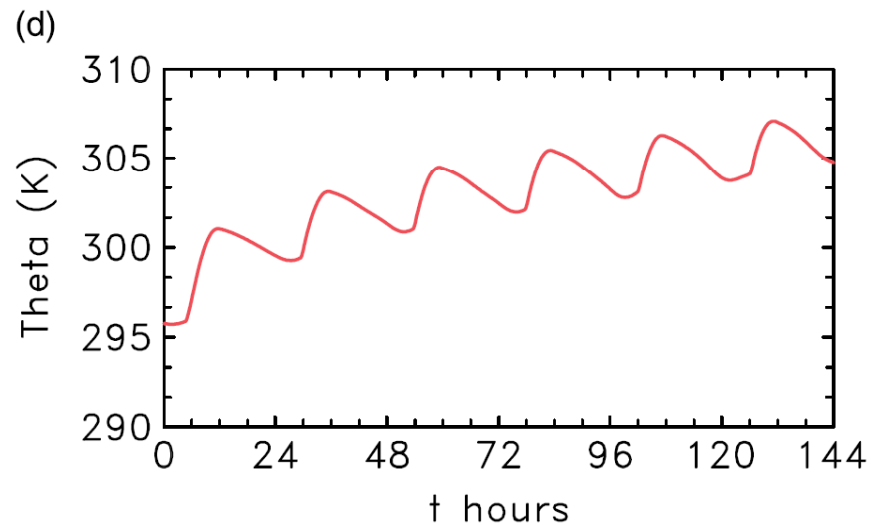
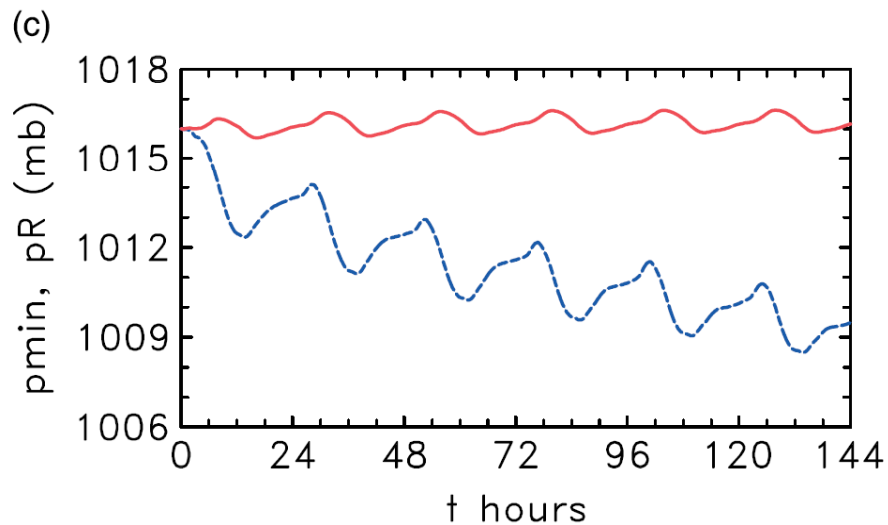
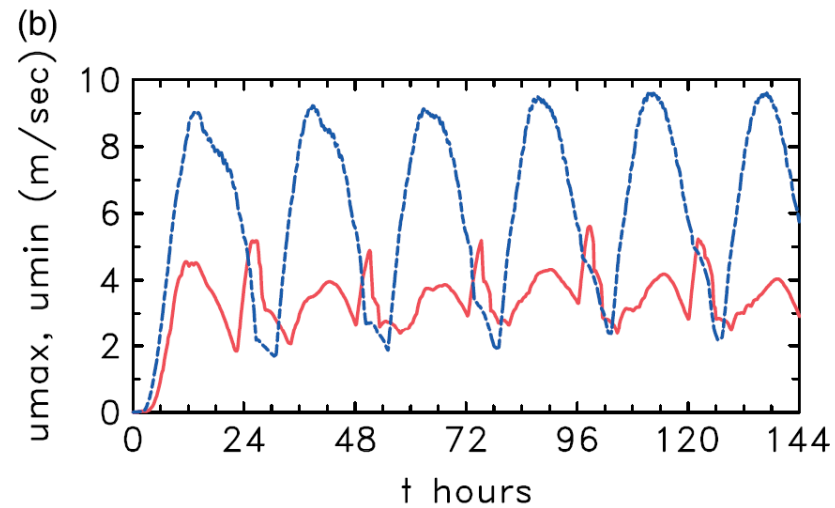
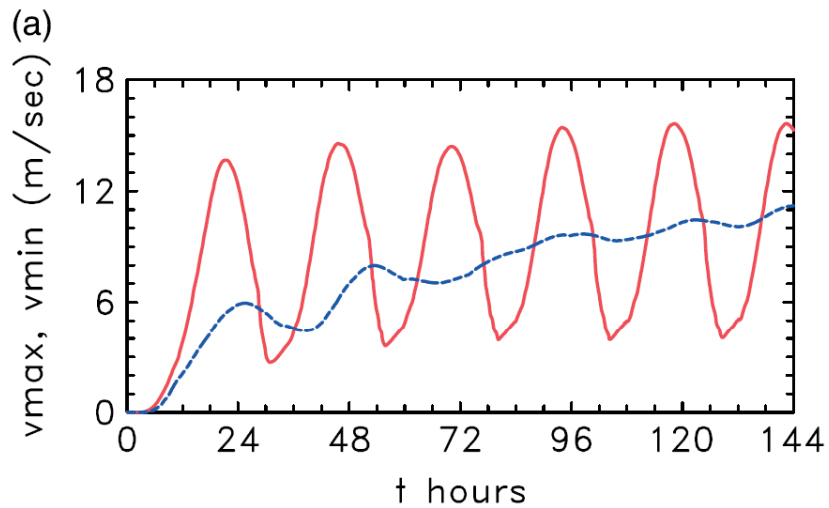
05.00 h



Solid lines - **outward**-, **dashed** lines - **inward**- pressure gradient force.

Spin-up

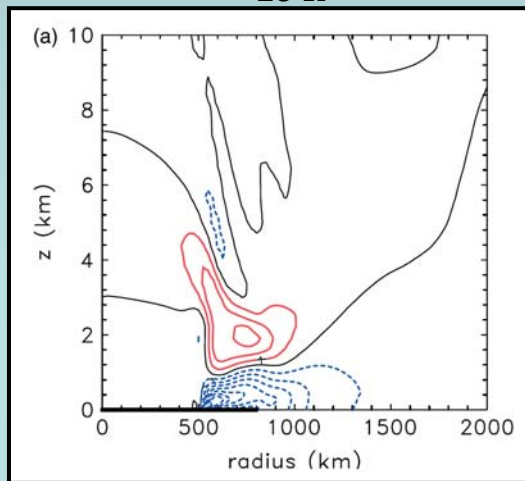
First 6 days



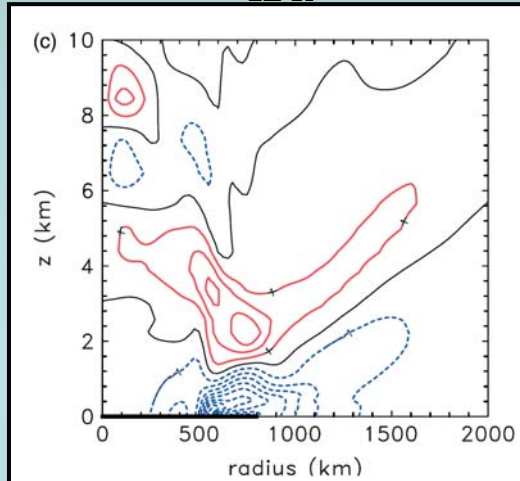
Spin-up

Vertical cross-sections of the radial (upper panels) and tangential (lower panels) wind components during first 3 days, contour interval 2 m/s

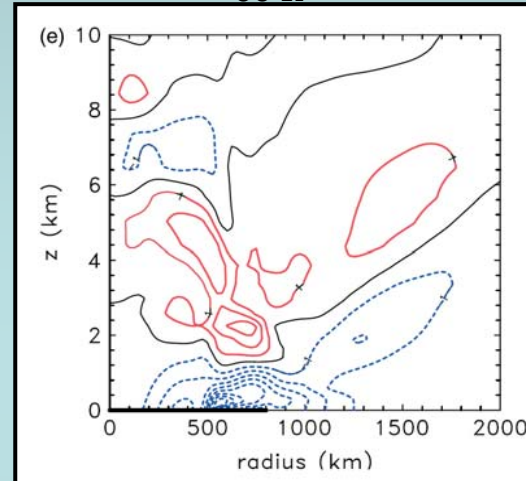
18 h



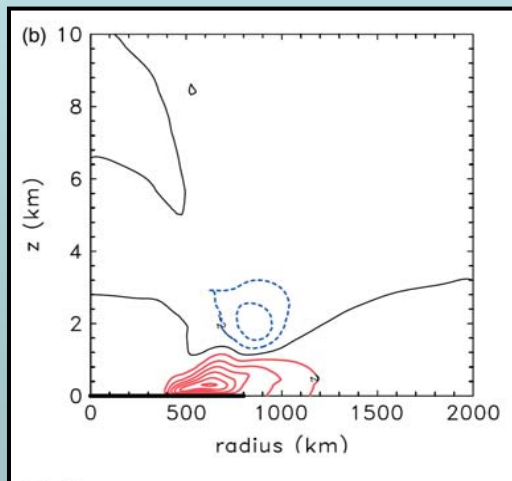
42 h



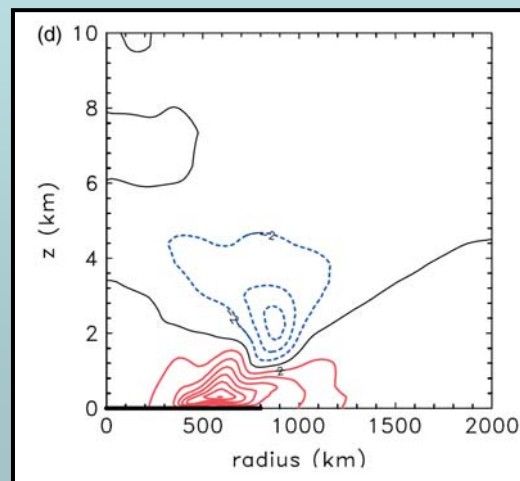
66 h



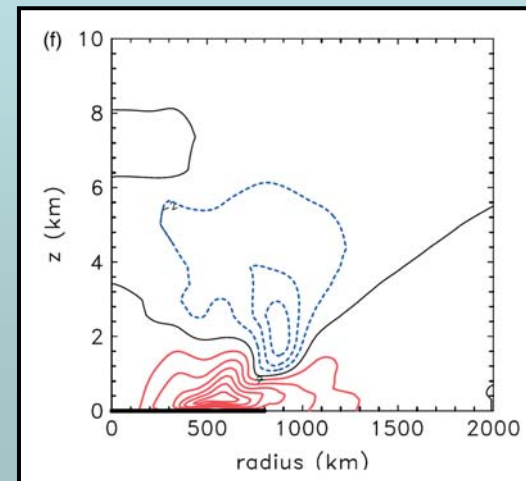
24 h



48 h



72 h



u

v

Inward
Outward

Az
Zn

Absolute Angular Momentum Budget

$$M = rv + \frac{1}{2} fr^2 \quad (11)$$

M - absolute angular momentum,
 r - radius,
 v - tangential wind speed,
 f - Coriolis parameter.

$$\frac{\partial M}{\partial t} + u \frac{\partial M}{\partial r} + w \frac{\partial M}{\partial z} = F \quad (12)$$

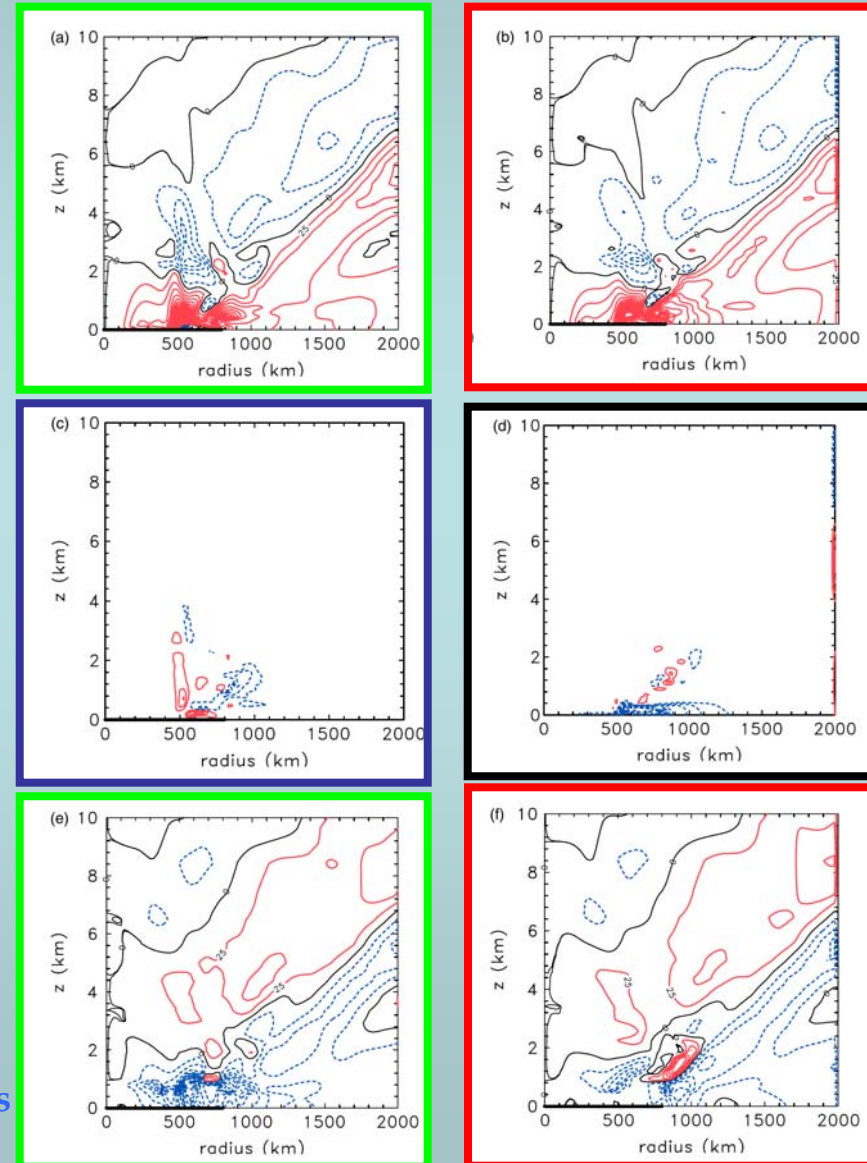
F - frictional torque.

00.00 h
Day 5

12.00 h
Day 5

Solid lines - gain, dashed lines - loss
of absolute angular momentum.

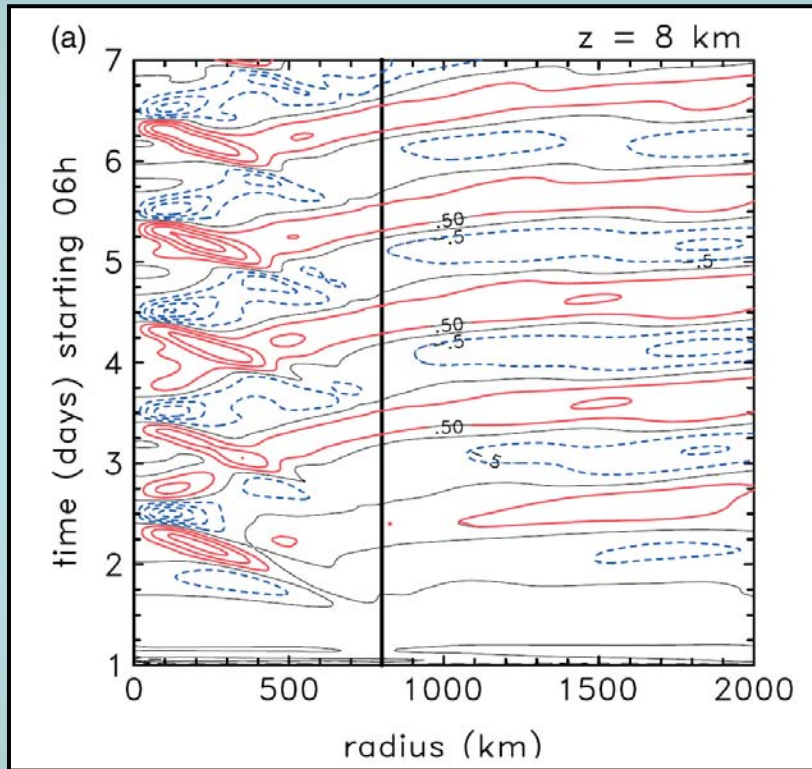
Absolute angular momentum tendency
Contour interval 25 m²/s²



Conclusions

1. Implementation of corrected and extended version of radiation scheme leads to a more realistic depth of the daytime mixed layer.
2. The upper-level anticyclone extends through much of the troposphere, but has a maximum strength in the lower troposphere.
3. The anticyclone develops steadily over a period of a few days and is associated with the return branch of sea-breeze circulation in lower troposphere and slow diurnal-mean outflow in the middle and upper troposphere.
4. The upper anticyclone is largely in gradient wind balance.
5. The gravity wave has a significant effect on the radial and vertical components of motion field at any one time.
6. In a mean sense we can distinguish between distinct patterns of the tangential flow component
 - between midnight and noon, when the low-level cyclone is strongest, and
 - between noon and midnight when it is much weaker.

Radial velocity, contour 0.5 m/s



Vertical velocity, contour 1 m/s

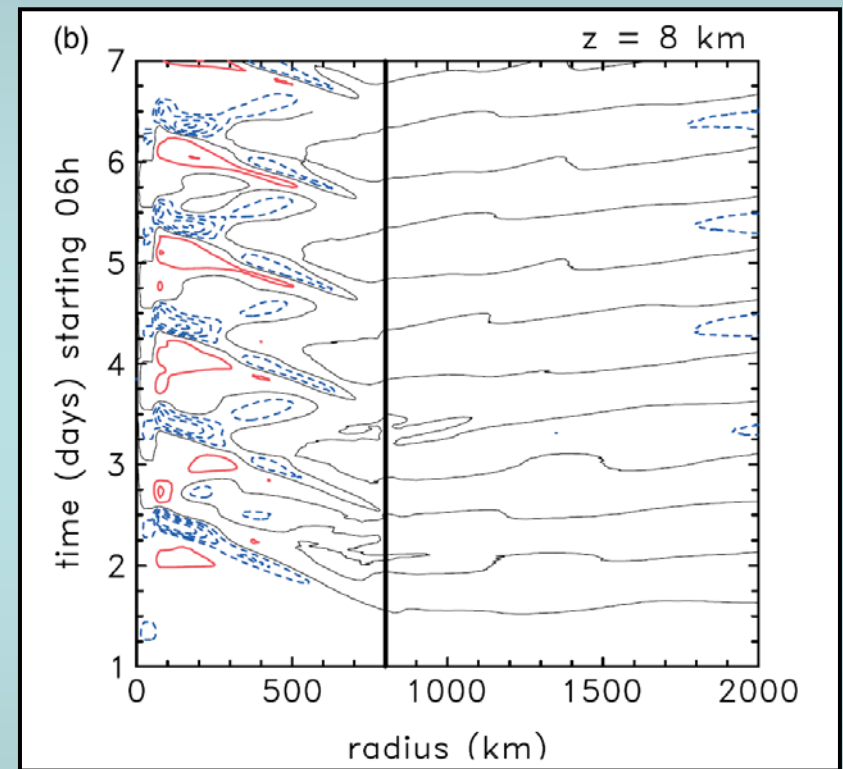


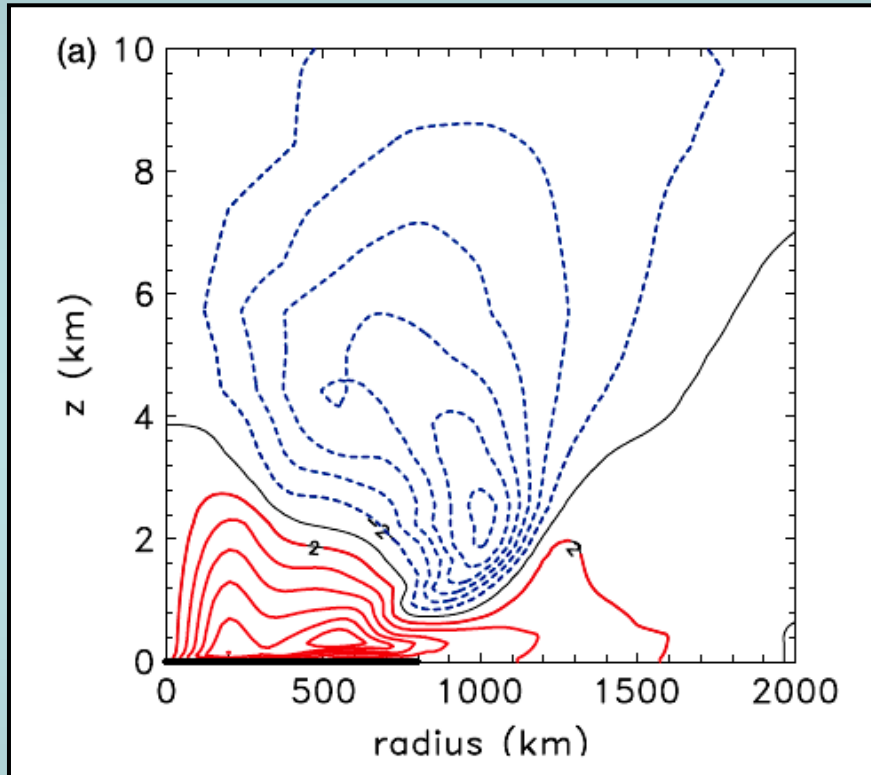
Figure 13. Hovmöller diagrams of (a) radial velocity, and (b) vertical velocity at a height of 8 km during the first six days of integration. The contour interval in (a) is 0.5 m s^{-1} , with solid lines indicating outward and dashed lines inward flow; the contour interval in (b) is 1 m s^{-1} , with solid lines indicating upward and dashed lines downward flow. The thick vertical line shows the position of the coast, with land to the left and sea to the right. This figure is available in colour online at www.interscience.wiley.com/journal/qj

Conclusions

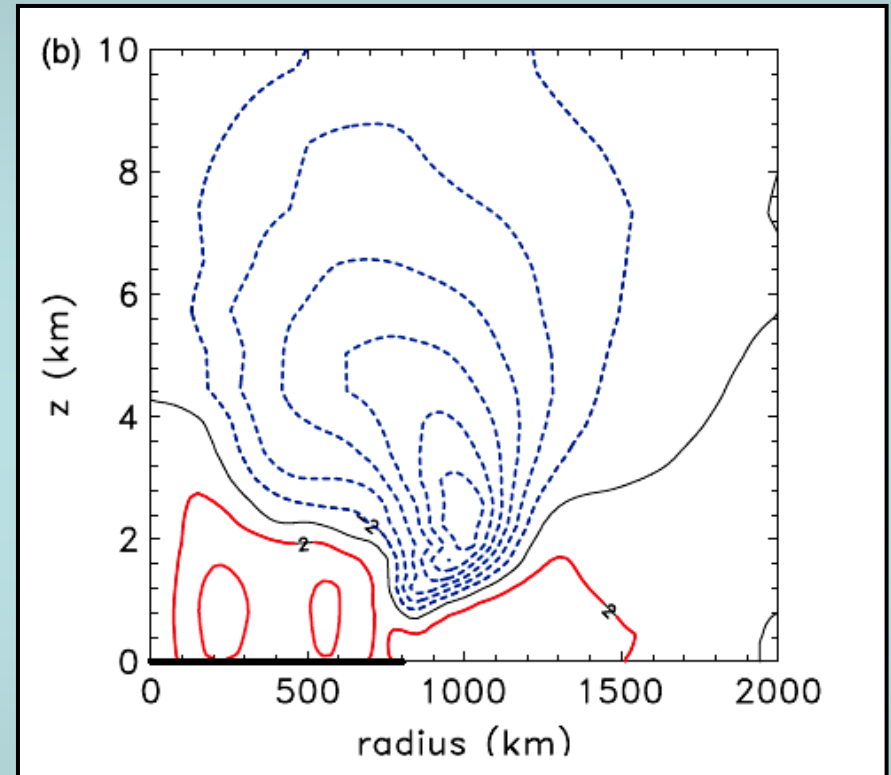
1. Implementation of corrected and extended version of radiation scheme leads to a more realistic depth of the daytime mixed layer.
2. The upper-level anticyclone extends through much of the troposphere, but has a maximum strength in the lower troposphere.
3. The anticyclone develops steadily over a period of a few days and is associated with the return branch of sea-breeze circulation in lower troposphere and slow diurnal-mean outflow in the middle and upper troposphere.
4. The upper anticyclone is largely in gradient wind balance.
5. The gravity wave has a significant effect on the radial and vertical components of motion field at any one time.
6. In a mean sense we can distinguish between distinct patterns of the tangential flow component
 - between midnight and noon, when the low-level cyclone is strongest, and
 - between noon and midnight when it is much weaker.

Impact of Radiation Scheme

6-hourly mean of tangential wind component, contour 2 m/s



[midnight <=> 06.00 h]

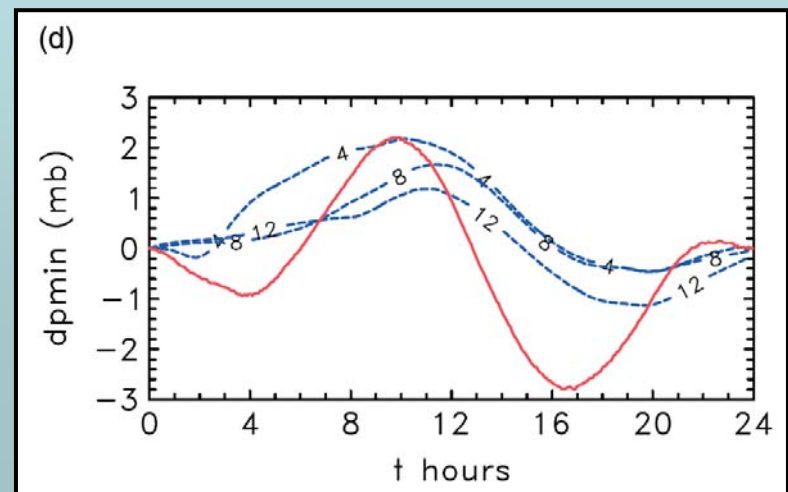
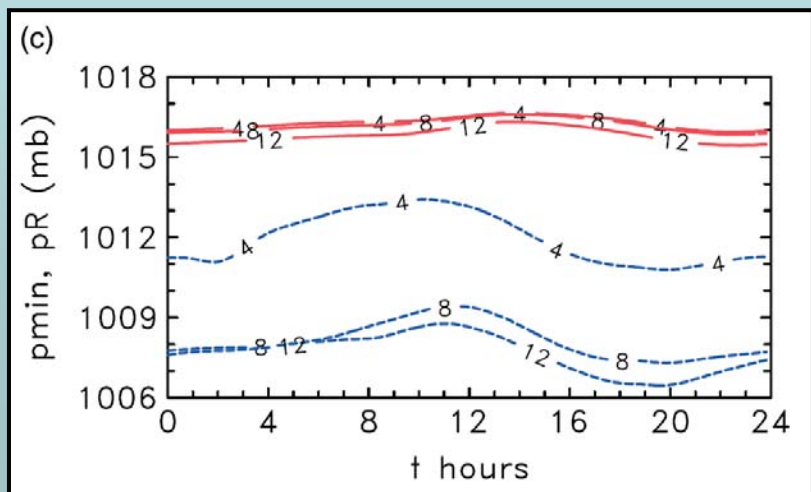
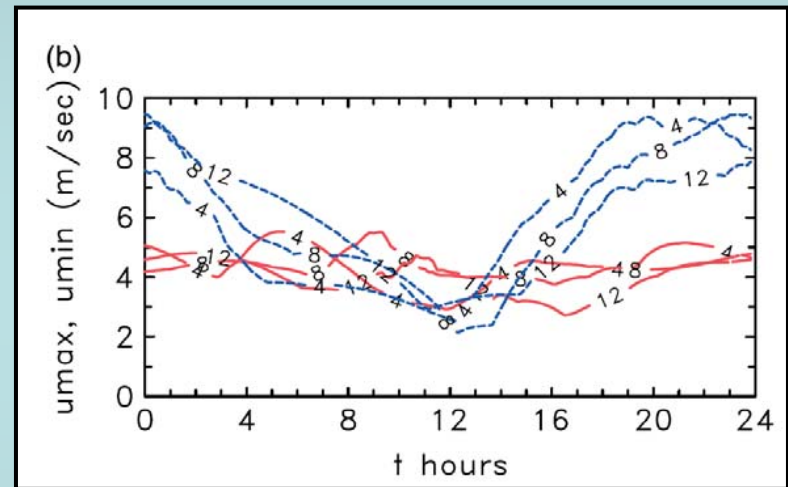
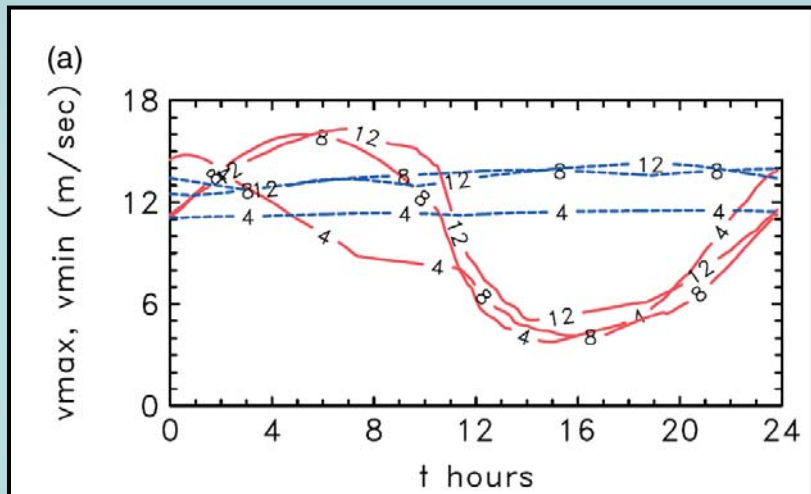


[noon <=> 18.00 h]

Solid lines - **Zn**, **dashed** lines - **Az** circulation.

The diurnal variation (mature stage - day 11) of
the strength of the heat low (v_{max}, p_{min}),
the strength of the upper-level anticyclone (v_{min}),
the strength of the maximum inflow (u_{min}),
the strength of the maximum outflow (u_{max}),
surface pressure on the domain boundary (pR).

4 => R = 400 km // 8 => R = 800 km // 12 => R = 1200 km



**Thanks for your
patience and attention !**